INTEGRATING BIOMASS TO PRODUCE HEAT AND POWER AT ETHANOL PLANTS

M. J. De Kam, R. V. Morey, D. G. Tiffany

ABSTRACT. *Several technology options are available that can help improve the sustainability of ethanol production from corn. Dry-grind ethanol process coproducts and other nearby biomass resources can be used to produce process heat and electricity at ethanol plants. These biomass fuels can reduce process energy costs, provide a consistent source of renewable electricity for the local utility, and increase the renewable energy balance for fuel ethanol production. An Aspen Plus model of the dry-grind ethanol process is used as a basis for the integration of biomass-fueled combined heat and power systems. Several combinations of combustion and gasification systems, power production cycles, biomass fuel combinations, and air emission control technologies are evaluated. Suitable configurations for incorporating biomass to produce heat and power at typical 190 million-L (50 million-gal) per year dry-grind ethanol facilities are analyzed.*

Keywords. *Biomass, Renewable, Sustainable, Model, Gasification, Combustion, Emissions, Ethanol production, Combined heat and power.*

The energy required to produce ethanol continues to be an important topic in the bio-fuel industry. Process energy in the form of heat and electricity is the largest energy input into the ethanol production process (Shapouri et al., 2002). Ethanol plants have a choice as to which fuel they will use to supply this energy. The most common source is currently natural gas. Some plants are being designed to use coal. Biomass is an alternative, renewable source of energy for ethanol plants. Dry-grind corn ethanol plants produce biomass coproducts which contain a significant amount of energy when used as a fuel. These ethanol plants also are typically located near corn producing areas which may have a large amount of corn stover available for use as a fuel. These biomass-powered dry-grind ethanol plants could generate the electricity they need for processing as well as surplus electricity to sell to the grid. Using biomass as a fuel replaces a large fossil fuel input with a renewable fuel input which will significantly improve the renewable energy balance of dry-grind corn ethanol (Morey et al., 2006).

Rausch and Belyea (2006) describe methods of processing corn including the dry-grind ethanol process. A generalized diagram of the conventional dry-grind ethanol process is shown in figure 1.

The ethanol coproduct streams include distillers wet grains (DWG), condensed solubles (syrup), and/or distillers dried grains with solubles (DDGS). Generally the syrup and DWG are mixed together and dried to make DDGS, which is sold as animal feed (Belyea et al., 2004; Rosentrater, 2006). The coproduct dryer is typically natural gas fired and demands a significant amount of energy.

Since under current production practices, most corn stover is left in the field, there are costs associated with collection, transportation, storage, and pre-processing to make the material into a convenient fuel. Sokhansanj and Turhollow (2004) estimate costs of corn stover at $60/t for large round bales and $80/t for densified (cubed) material.

OBJECTIVES

The main objective of this analysis is to model the technical integration of several biomass energy conversion systems into the dry-grind corn ethanol process. Mass and energy balances are performed for each conceptual system design to determine fuel use and performance. Air pollutant emissions estimates are calculated and the renewable energy balance of ethanol production is evaluated for each system.

METHODS

The heat and power generation systems are integrated into the dry-grind ethanol process and modeled using Aspen Plus process simulation software. The technology combinations are defined with advice from the engineering consulting firms RMT, Inc. (Madison, Wis.) and AMEC E&C Services Inc. (Minneapolis, Minn.), who are partners in this project. The following descriptions give an overview of the basis for the models as well as the methods used for modeling these systems in Aspen Plus.

ETHANOL PROCESS

An Aspen Plus model of the dry-grind ethanol process obtained from the USDA Agricultural Research Service

The authors are **Matthew J. De Kam, ASABE Member Engineer,** Graduate Student, **R. Vance Morey, ASABE Fellow,** Professor, Department of Bioproducts and Biosystems Engineering, University of Minnesota, St. Paul, Minnesota; and **Douglas G. Tiffany,** Research Fellow, Department of Applied Economics, University of Minnesota, St. Paul, Minnesota. **Corresponding author:** R. Vance Morey, Department of Bioproducts and Biosystems Engineering, University of Minnesota, 1390 Eckles Ave., St. Paul, MN 55108, phone: 612-625-8775; fax 612-624-3005; e-mail: rvmorey@umn.edu.
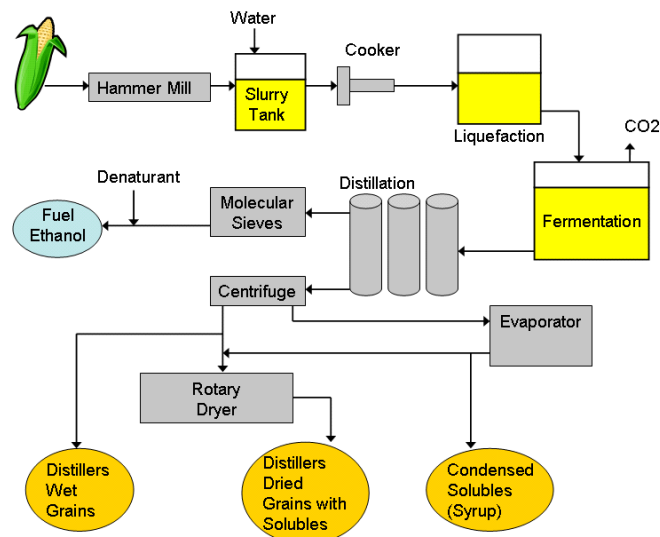
Figure 1. Conventional natural gas fired dry-grind ethanol process.

(ARS) serves as the basis for the energy conversion systems (McAloon et al., 2000; 2004; Kwiatkowski et al., 2006). This model contains a feature that allows it to be scaled to different annual ethanol outputs. For the purposes of this study all cases are set to produce 190 million L (50 million gal) per year of denatured ethanol. The primary components of the process such as fermentation, distillation, and evaporation are not changed. Only those components impacted by using biomass fuel are modified. They include steam generation (biomass combustion or gasification), thermal oxidation, and coproduct drying.

Table 1 shows the process steam energy demands for the ARS model. An additional process steam heat loss of 655 kW is assumed for the biomass steam generation cases to account for losses during steam distribution (Wang et al., 2007). This corresponds to 1% of the fuel energy input for a conventional plant bringing the process steam energy demands to a total of 27,890 kW. All of the biomass heat and power systems are modeled using this steam energy demand.

Table 1. Ethanol process energy demands.[a]

Process Steam Point of Use	Heat Duty (kW)	(% of total)
Process condensate exchanger	6,446	24
Cook heat exchanger	1,634	6
Beer column re-boiler	15,709	58
Stripper column re-boiler	3,054	11
Molecular sieve	392	1
Totals	27,235	100

[a] All values are for a 190M L (50MM gal) per year plant.

An important objective of this study is to evaluate the renewable energy ratio of ethanol production under the new biomass energy systems. The renewable energy ratio for each case is calculated following the assumptions used by Morey et al. (2006). The renewable energy ratio (RER) is defined as follows:

$$RER = (\text{Energy in Ethanol} + \text{Coproduct Energy} + \text{Electricity to Grid Energy})/(\text{Fossil Energy Input}) \quad (1)$$

The energy use and credit assumptions used are shown in table 2. When electricity is produced from a biomass fuel and sold to the grid it is assumed that this renewable electricity will displace fossil sources of electricity. It is assumed that on average fossil-based electricity is generated at an efficiency of 35% on a Lower Heating Value (LHV) basis.

BIOMASS PROPERTY DATA

A typical dry-grind corn ethanol plant produces distiller's dried grains with solubles (DDGS) as a coproduct. DDGS is a mixture of two process streams called distiller's wet grains (DWG) and concentrated distiller's solubles (also known as "syrup"). The DWG and syrup are mixed and dried together to become DDGS. Property data for these process streams and corn stover is needed in order to build an accurate model. Morey et al. (2009) provide an analysis of the fuel properties of these streams based on data taken from five dry-grind ethanol plants, as well as a fuel characterization of corn stover. Table 3 provides a summary of some of the important biomass property data.

Table 2. Technical assumptions for energy use in the dry-grind ethanol process.[a]

Category	Energy Use	Source
Fossil energy for corn production	6.27 MJ/L (22,500 Btu/gal)	Shapouri et al. (2004)
Natural gas for process heat	8.26 MJ/L (29,600 Btu/gal)	ARS Model
Ethanol process electricity demand	2.04 MJ/L (0.75 kWh/gal)	EPA (2007)
Fossil energy for corn stover production and processing	0.82 MJ/kg (354 Btu/lb)	Morey et al. (2006)
Energy in ethanol	21.3 MJ/L (76,330 Btu/gal)	Shapouri et al. (2004)
Ethanol coproduct energy credit	7.38 MJ/L (26,482 Btu/gal)	Shapouri et al. (2004)

[a] Energy values in this table are based on the Lower Heating Value (LHV).

Fuel	Moisture Content (% wet basis)	HHV[b] (MJ/kg dry matter)	Nitrogen (% dry Matter)	Sulfur (% dry Matter)	Chlorine (% dry Matter)
Corn stover	13	17.9	0.7	0.04	0.1
Syrup	67	19.7	2.6	1.0	0.35
DDGS	10	21.8	4.8	0.8	0.18
DWG	64	22.0	5.4	0.7	0.17

[a] Morey et al. (2009).
[b] HHV (Higher Heating Value) - corresponding Lower Heating Value (LHV): 16.7, 18.2, 20.2, and 20.5 MJ/kg dry matter for corn stover, syrup, DDGS, and DWG, respectively.

In Aspen Plus the biomass fuels are represented as solid non-conventional components. The ultimate analysis of each fuel is used to provide the necessary data for the general enthalpy and general density property models in Aspen Plus which allow the user to enter density, specific heat capacity, and enthalpy of formation values for each component manually. Wooley and Putche (1996) define a specific heat capacity of 1.545 kJ/kg-K for biomass, and this value is used for all the fuels during modeling. The Redlich-Kwong-Soave (RKS) equation of state with Boston-Mathias alpha function is used as the thermodynamic property method in Aspen Plus (Soave, 1972). This equation of state is recommended by the makers of Aspen Plus for simulations involving combustion and power generation. Details of the modeling using the RKS equation are found in De Kam (2008).

COPRODUCT DRYING

Conventional dry-grind ethanol plants generally use natural gas direct-fired dryers (rotary or ring type) to dry the DDGS. During the drying process some Volatile Organic Compounds (VOCs) are produced, so the dryer exhaust stream must be treated by thermal oxidation at high temperature before release to the atmosphere (EPA, 2005). The natural gas required for drying is a major portion of the ethanol plant's energy needs. In the ARS ethanol plant model the dryer requires 43% of the total natural gas supplied to the plant (McAloon et al., 2004).

A goal of using biomass for energy is to eliminate the need for natural gas, so different dryers will need to be used. In a plant powered by solid fuel, a common option is to use steam tube (indirect heat) rotary dryers. In this setup steam from the boiler provides heat to the wet material and air in the dryer through a series of tubes arranged inside the rotating dryer cylinder (Perry et al., 1997). Steam tube dryers are used in each of the scenarios evaluated in this study. Data on dryer performance is provided by Davenport Dryer Company (Anon., 2008).

The Aspen Plus model of the dryer is shown in figure 2. The wet biomass materials (DWG and syrup in this case) enter mixed together at 67°C (152°F). Part of the moisture portion of the non-conventional component representing the biomass materials in Aspen Plus is converted to conventional liquid H_2O in the RSTOIC block. Ambient air at 100 kPa, 25°C, and 50% relative humidity enters the dryer. The amount of ambient air required is calculated based on the assumption that the exiting dryer exhaust has a humidity ratio of 0.75 kg water/ kg dry air as suggested by Davenport Dryer Co. The water is evaporated in a countercurrent heat exchanger block using process steam as a heat source. The heat exchanger is specified so that the biomass and exhaust exit at a temperature of 90.6°C (195°F). A small heat loss is modeled in the condensate return line and is assumed as 2% of the dryer thermal load. A FLASH2 block is used to separate the exhaust vapors from the biomass material. Dried product (DDGS) exits the dryer at 10% moisture.

THERMO-CHEMICAL CONVERSION

Fluidized bed combustion and gasification are the main thermal conversion options evaluated in this study. Fluidized bed combustion is a good candidate because of its capacity to utilize high moisture fuels and the option of adding limestone as a bed material to control emissions. Fluidized bed gasification has the added benefits of lower operating temperatures which is important because of the low ash fusion temperatures of DDGS. Gasification also permits greater control of the conversion process through the option of synthesis gas cleanup before subsequent combustion.

Fluidized Bed Combustion

The combustion process in Aspen Plus is modeled as a bubbling fluidized bed combustor (BFBC). Figure 3 shows a diagram of the Aspen Plus combustion model including
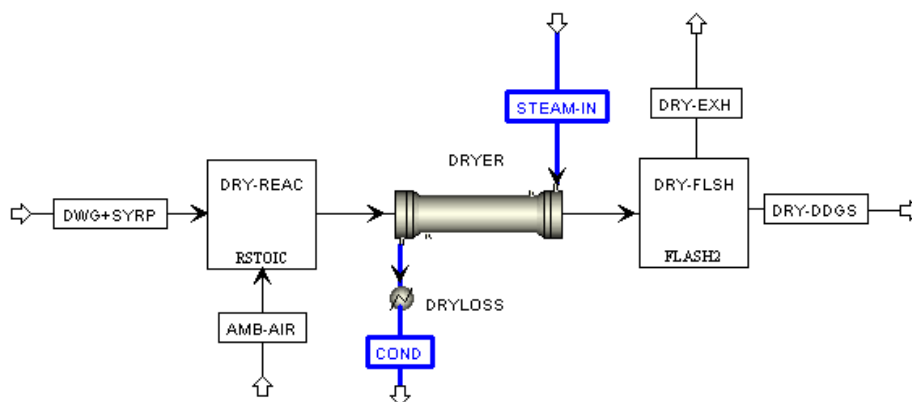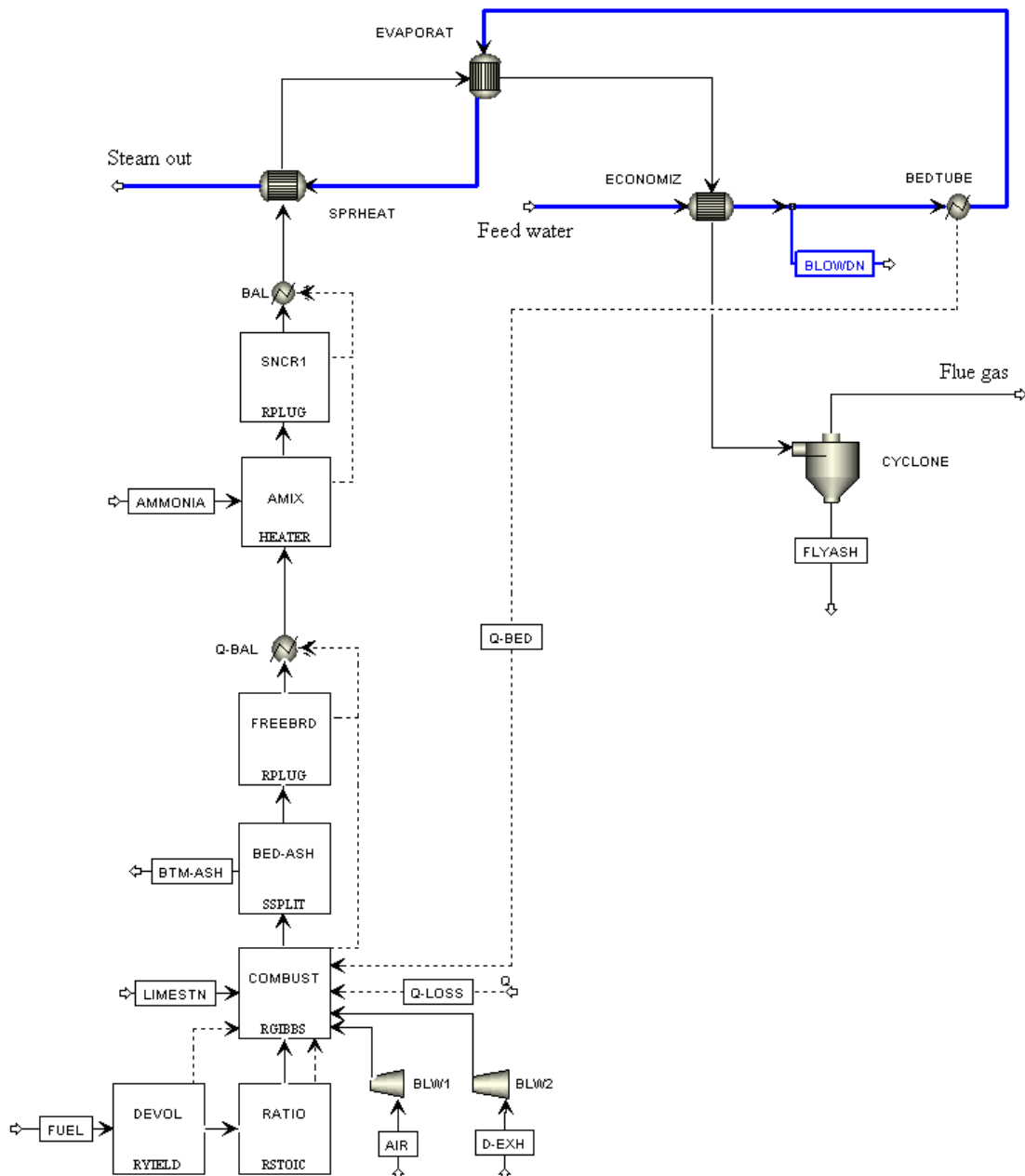

Figure 2. Aspen Plus model of the steam tube dryer.

Figure 3. Aspen Plus model for the bubbling fluidized bed combustor.

emissions control and boiler models. At the base of the combustor ambient air and the exhaust stream from the coproduct dryer serve as the means of bed fluidization. The combustor operates at nominally atmospheric pressure, but in order to keep the bed particles in a fluidized state the velocity and pressure of the air and dryer exhaust streams must be increased by blowers. The pressure drop across the bed is estimated to be 12 kPa based on industry data. The centrifugal turbo blowers are modeled as an adiabatic compression process with an isentropic efficiency of 70%, and a mechanical efficiency of 95% for the driving motor. The dryer exhaust stream is compressed separately from the air stream because of its high relative humidity. This avoids significant cooling of the dryer exhaust which would almost certainly result in condensation during the compression process.

As the biomass fuel enters the combustor it is devolatilized instantaneously into carbon, hydrogen, oxygen, sulfur, chlorine, ammonia, and hydrogen cyanide (Ngampradit et al., 2004; Khan et al., 2007). This is accomplished in Aspen Plus using an RYIELD block which converts the biomass based on its ultimate analysis, followed by an RSTOICH block to control the ratio of ammonia (NH_3) to hydrogen cyanide (HCN). All fuel nitrogen is assumed to devolatilize as NH_3 or HCN. It is commonly assumed in biomass combustion models that most fuel nitrogen will form NH_3 with a very small portion forming HCN (Liu and Gibbs, 2003; Khan et al., 2007). Here it is assumed 5% of the fuel nitrogen forms HCN and the remaining 95% forms NH_3 during devolatilization based on the work of Liu and Gibbs (2003) who assumed 90% of fuel nitrogen forms NH_3 and

Khan et al. (2007) who assumed 100% of fuel nitrogen forms NH_3.

Volatile combustion occurs in the next stage of the combustion model. The air and dryer exhaust streams react with the devolatilized biomass fuel and the limestone bed material in the fluidized bed. Limestone is modeled as $CaCO_3$ and is added to the bed at a Ca/S molar ratio of 3.0 relative to the fuel sulfur. The combustor is operated with 35% excess O_2 taking into account the oxygen available in both the dryer exhaust and ambient air streams (Black and Veatch, 1996). An RGIBBS reactor is used in Aspen Plus to perform an equilibrium calculation according to the chemical reaction set shown in table 4.

For this system-level analysis an equilibrium model is used with a temperature approach to equilibrium specified for certain key reactions. This effectively changes the temperature at which the equilibrium constant is calculated for the specified reaction so that the model conforms more closely to the results of empirical studies. A temperature approach to equilibrium is specified for reaction 10 because of its importance in determining the amount of sulfur captured by the bed sorbent material (Black and Veatch, 1996). Reaction 11 also has a specified temperature approach to equilibrium on account of its importance to the amount of chlorine captured by the bed sorbent material (Coda et al., 2001).

Although BFBCs typically recycle the fly ash back into the bed, some of the fuel carbon is removed from the bed with the bottom ash before reacting. A carbon loss of 2% is assumed in this model, and the lost carbon passes through the reactor to be removed with the ash (Radovanović, 1986). NH_3 and HCN are also passed through the bed reactor to be dealt with in the freeboard section of the combustor. Part of the limestone bed material is calcined to quicklime (CaO) in the bed according to reaction 9 and the CaO subsequently reacts to absorb sulfur and chlorine. The excess limestone and quicklime as well as the solid products of the sorbent reactions (10 and 11) are removed with the ash.

Heat is removed from the bed by boiler tubes which are immersed in the fluidized material. These heat exchange tubes are represented in Aspen Plus by a heat stream connecting the equilibrium reactor and a heater block in the steam generation section. The combustor is modeled without water-cooled walls, and heat loss from the skin of the combustor is calculated using a correlation based on the capacity of the unit by the American Boiler Manufacturers Association as presented in Babcock and Wilcox Co. (1992).

In the next section of the combustion model homogeneous gas phase reactions involving NH_3 and HCN from fuel nitrogen are considered using a kinetic model. Physically these reactions would be taking place mainly in the freeboard above the bed and also in the bubble phase of the bed. The fuel NO_x mechanism shown in table 5 is used in a plug flow reactor. The plug flow assumption is commonly used for homogeneous gas phase reactions in fluidized bed combustion models (Liu and Gibbs, 2002; de Souza-Santos, 2004; Khan et al., 2007).

Reactions 12 and 13 are the same fuel NO_x reactions used in a biomass fluidized bed combustion model by Khan et al. (2007). Reaction 14 is adapted from a reaction scheme in Deroches-Ducarne et al. (1998) which allows HCN to produce either NO or N_2O, both of which are regulated air pollutants. Here only NO is considered and it is assumed that all HCN will form NO according to the kinetics of the relatively slow HCN oxidation reaction as shown in table 6.

Thermal NO_x reactions are not considered in this model as the combustion temperatures are in the range of 1173 to 1200 K. This is well below the threshold of 1800 K where it is suggested that thermal NO_x begins to be significant (Annamalai and Puri, 2007). The combustion reactions occurring in the fluidized bed and in the freeboard above the bed are considered to be isothermal as is the assumption in a similar Aspen Plus fluidized bed combustor model by Ngampradit et al. (2004). In Aspen Plus all the combustion reaction blocks are connected by heat streams and are set at the specified temperature. The heat streams terminate and are balanced in a heater block above the freeboard. The resulting temperature in this heat balance block is adjusted to match the specified combustion temperature by changing the amount of heat removed by the bed boiler tubes.

Table 4. Equilibrium combustion reaction set.

No.[a]	Reaction
1	$2H_2 + O_2 \Leftrightarrow 2H_2O$
2	$N_2 + 2O_2 \Leftrightarrow 2NO_2$
3	$N_2 + O_2 \Leftrightarrow 2NO$
4	$S + O_2 \Leftrightarrow SO_2$
5	$2S + 3O_2 \Leftrightarrow 2SO_3$
6	$2C + O_2 \Leftrightarrow 2CO$
7	$C + O_2 \Leftrightarrow CO_2$
8	$Cl_2 + H_2 \Leftrightarrow 2HCl$
9	$CaCO_3 \Leftrightarrow CaO + CO_2$
10	$2CaO + 2SO_2 + O_2 \Leftrightarrow 2CaSO_4$
11	$CaO + 2HCl \Leftrightarrow CaCl_2 + H_2O$

[a] 1-7: Annamalai and Puri (2007).
9, 10: Black and Veatch (1996).
11: Coda et al. (2001).

Table 5. Fuel NOx mechanism.

No.[a]	Reaction
12	$NH_3 + \frac{5}{4}O_2 \rightarrow NO + \frac{3}{2}H_2O$
13	$NH_3 + NO + \frac{1}{4}O_2 \rightarrow N_2 + \frac{3}{2}H_2O$
14	$HCN + \frac{5}{4}O_2 \rightarrow NO + \frac{1}{2}H_2O + CO$

[a] 12,13: Khan et al. (2007).
14: Deroches-Ducarne et al. (1998).

Table 6. Fuel NOx mechanism kinetic parameters.[a]

No.[b]	Rate Expression	Parameter (k)
12	$k[NH_3][O_2]$	$5.07 \times 10^{14} \exp(-35230/T)$
13	$k[NH_3]^{0.5}[NO]^{0.5}[O_2]^{0.5}$	$1.11 \times 10^{12} \exp(-35230/T)$
14	$k[HCN][O_2]$	$2.14 \times 10^5 \exp(-10000/T)$

[a] All parameters are in SI units. Concentrations have units of $[mol/m^3]$.
[b] 12, 13: Khan et al. (2007).
14: Deroches-Ducarne et al. (1998).

Fluidized Bed Gasification

The partial oxidation gasification process is modeled in Aspen Plus under isothermal conditions at near atmospheric pressure using ambient air as the gasification media. A diagram of the Aspen Plus gasification model is shown in figure 4.

Ambient air passes through a blower and is raised from 100 to 118.6 kPa before serving as the fluidization and gasification media. The centrifugal turbo blower is modeled as an adiabatic compression process with an isentropic efficiency of 70% and a mechanical efficiency of 95% for the driving motor.

The DDGS biomass fuel is initially devolatilized into its constituent components in an RYIELD block similar to the approach taken in Nikoo and Mahinpey (2008). Next, the gas distribution is shifted in an RSTOIC block according to the assumptions that all fuel sulfur will initially produce H_2S and all fuel chlorine will initially produce HCl. The partitioning of fuel nitrogen is also set at this stage similar to the assumption made in Liu and Gibbs (2003). Five percent of the fuel nitrogen produces HCN with the remaining nitrogen forming NH_3.

The reactions between the biomass, gasifying air, and limestone bed material are evaluated in the next stage of the gasification model. An equilibrium RGIBBS reactor is used in Aspen Plus to model the gasification reactions according to the reaction set shown in table 7. Limestone is modeled as $CaCO_3$ and enters the bed at a Ca/S molar ratio of 2.5 relative to the fuel sulfur.

The detailed reaction mechanisms that occur during gasification are complex and the kinetic parameters are still being explored by many researchers (Chejne and Hernandez, 2002; Higman and van der Burgt, 2003; de Souza-Santos, 2004). In many cases an equilibrium model of the gasification process can provide an adequate representation (Ruggiero and Manfrida, 1999; Higman and van der Burgt, 2003; Melgar et al., 2007). An equilibrium model is used in this case. Temperature approaches to equilibrium are specified for certain reactions, and the production of certain species is set based on the amount of fuel being used. In
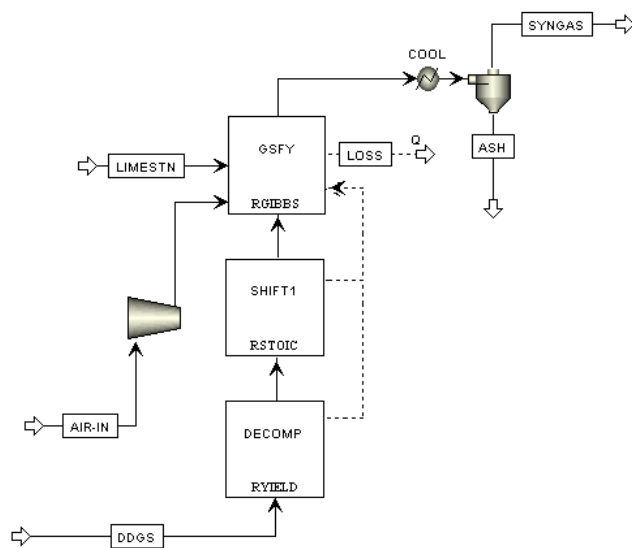
Table 7. Equilibrium gasification reaction set.

No.[a]	Reaction
15	$C + O_2 \Leftrightarrow CO_2$
16	$C + H_2O \Leftrightarrow CO + H_2$
17	$CO + 3H_2 \Leftrightarrow CH_4 + H_2O$
18	$CO + H_2O \Leftrightarrow CO_2 + H_2$
19	$\frac{1}{2}CO + H_2 \Leftrightarrow C_2H_4 + \frac{1}{2}H_2O$
20	$C + \frac{1}{2}H_2 \Leftrightarrow \frac{1}{6}C_6H_6$
21	$CaCO_3 \Leftrightarrow CaO + CO_2$
22	$CaO + H_2S \Leftrightarrow CaS + H_2O$
23	$CaO + 2HCl \Leftrightarrow CaCl_2 + H_2O$

[a] 15: Turns (2000).
16-18: Higman and van der Burgt (2003).
21, 22: Yrjas et al. (1996).
23: Weinell et al. (1992).

reaction 15 a portion of the fuel carbon is combusted to provide heat needed in the gasification process. Reaction 16 is sometimes referred to as the water gas reaction where water reacts with carbon at high temperatures to produce combustible gas (Higman and van der Burgt, 2003). Steam methane reforming is represented by reaction 17, and the production of methane is set as a ratio of the fuel being gasified (Klass, 1998; Higman and van der Burgt, 2003). Reaction 18 is the water gas shift reaction and is specified with a temperature approach (Higman and van der Burgt, 2003).

The production of ethylene and benzene (tar) is controlled by reactions 19 and 20, respectively, and is set based on the amount of fuel being gasified. Reactions 21 through 23 represent the calcination of limestone and subsequent absorption of HCl and H_2S. The absorption reactions are specified with temperature approaches due to their importance in determining emissions values (Duo et al., 1996; Yrjas et al., 1996). The equilibrium reactor does not change the amounts of NH_3 and HCN to maintain the original assumption about fuel nitrogen partitioning. Four percent of the fuel carbon is assumed to exit the gasifier as solid char based on estimates from our research partner RMT Inc, and a Department of Energy biomass gasification benchmarking study (Ciferno and Marano, 2002; Morey et al., 2009).

All stages in this gasification model are isothermal at a specified temperature of 750°C, and the heat loss from the gasifier is represented by a heat loss stream from the equilibrium reactor block. A heater block is used to model an assumed cooling of the synthesis gas by 110°C as it passes through the cyclone and over to the combustion unit. All solids are removed from the producer gas in the cyclone including ash, char, excess limestone, and the solid products of absorption reactions.

Synthesis Gas Combustion

The synthesis gas combustion happens in two stages. In the first stage primary air reacts with the synthesis gas in a combustion tube. In the second stage additional air completes
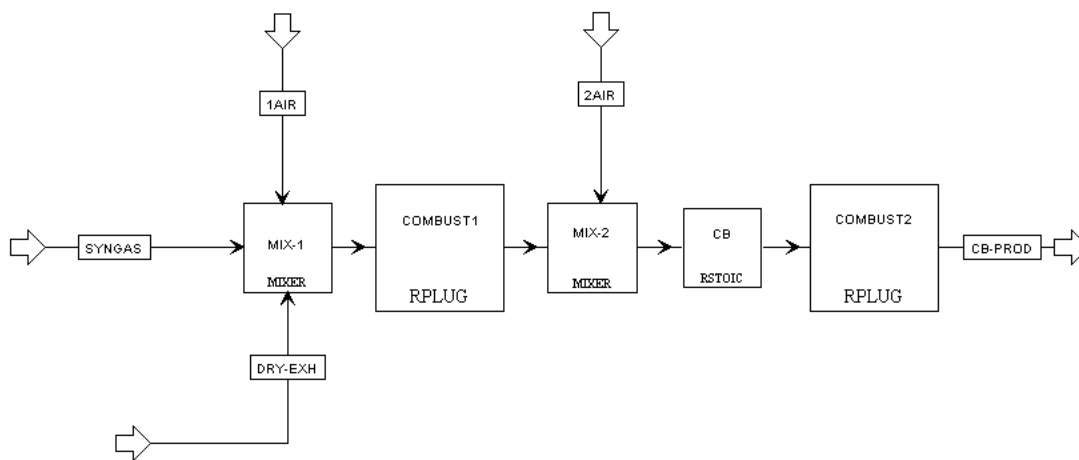

Figure 4. Aspen Plus model of fluidized bed gasification.

Figure 5. Aspen Plus model of staged synthesis gas combustion.

the combustion of synthesis gas. A diagram of this two stage configuration is shown in figure 5.

Synthesis gas is initially mixed with the humid dryer exhaust stream and some ambient air. This mixture is then combusted in an adiabatic plug flow reactor according to the reaction set presented in table 8. This set of homogeneous gas phase reactions occurs under fuel rich conditions in the primary combustion tube. The reactions proceed quickly according to the kinetic parameters in table 9 until all oxygen is reacted.

In the second stage of the synthesis combustion process secondary combustion air is added to complete the reaction. All H_2S is converted to SO_2 in this stage. The secondary combustion reaction occurs in an adiabatic plug flow reactor according to the same reaction set presented in tables 8 and 9. The overall combustion process is supplied with 5% excess oxygen taking into account the oxygen supplied by the dryer exhaust stream.

EMISSIONS CONTROL

Emissions estimates and technology specifications are made using data from the literature on emissions control technology and suggestions from the partner engineering firms. This information along with emissions modeling is used to develop emissions control equipment specifications for each case. Additional details of the emissions modeling are found in De Kam (2008).

NOx Emissions

Emissions of NO_x are controlled using selective non-catalytic reduction (SNCR). For combustion systems with SNCR, ammonia is injected into the flue gases to achieve NO_x reduction. In the case of gasification, ammonia produced during gasification can assist with NO_x reduction if the synthesis gas is burned in a carefully designed staged combustion reactor. Additional ammonia is injected in the combustion flue gas (SNCR) to further reduce NO_x.

In Aspen Plus the SNCR process is modeled using an isothermal plug flow reactor as shown in figure 6. The

Table 8. Synthesis gas combustion reactions.

No.[a]	Reaction
24	$C_2H_4 + 3O_2 \Leftrightarrow 2CO_2 + 2H_2O$
25	$C_6H_6 + 7.5O_2 \Leftrightarrow 6CO_2 + 3H_2O$
26	$CH_4 + \frac{3}{2}O_2 \Leftrightarrow CO + 2H_2O$
27	$CO + \frac{1}{2}O_2 \Leftrightarrow CO_2$
28	$H_2 + \frac{1}{2}O_2 \Leftrightarrow H_2O$
29	$NH_3 + NO + \frac{1}{4}O_2 \rightarrow N_2 + \frac{3}{2}H_2O$
30	$NH_3 + \frac{5}{4}O_2 \rightarrow NO + \frac{3}{2}H_2O$
31	$HCN + \frac{5}{4}O_2 \rightarrow NO + \frac{1}{2}H_2O + CO$

[a] 24, 25: Turns (2000).
   26-30: Khan et al. (2007).
   31: Deroches-Ducarne et al. (1998).

Table 9. Synthesis gas combustion kinetic parameters.[a]

No.[b]	Rate Expression	Parameter (k)
24[c]	$k[C_2H_4]^{0.1}[O_2]^{1.65}$	$2.0 \times 10^{12} \exp(-15098/T)$
25[c]	$k[C_6H_6]^{-0.1}[O_2]^{1.85}$	$2.0 \times 10^{11} \exp(-15098/T)$
26	$k[CH_4][O_2]^{0.8}$	$1.547 \times 10^8 \exp(-15098/T)$
27	$k[CO][O_2]^{0.5}[H_2O]^{0.5}$	$1.585 \times 10^{10} \exp(-24157/T)$
28	$k[H_2]^{0.1}[O_2]$	$1.631 \times 10^9 \exp(-3420/T)$
29	$k[NH_3]^{0.5}[NO]^{0.5}[O_2]^{0.5}$	$1.11 \times 10^{12} \exp(-27680/T)$
30	$k[NH_3][O_2]$	$5.07 \times 10^{14} \exp(-35230/T)$
31	$k[HCN][O_2]$	$2.14 \times 10^5 \exp(-10000/T)$

[a] All parameters are in SI units with concentrations in [mol/m³] unless otherwise noted.
[b] 24, 25: Turns (2000).
   26-30: Khan et al. (2007).
   31: Deroches-Ducarne et al. (1998).
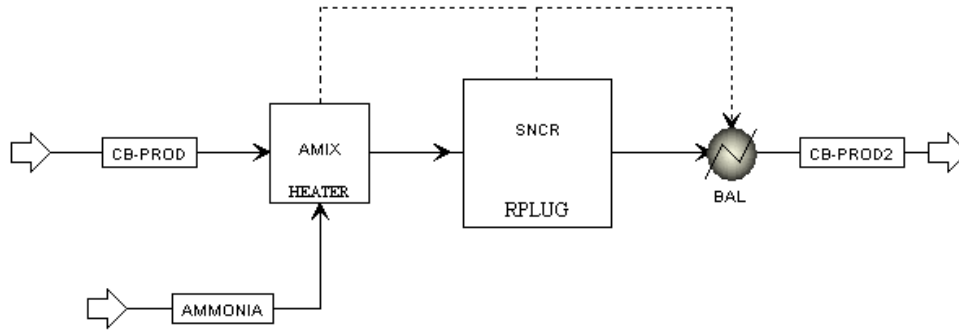[c] Concentrations in [mol/cm³] for reactions 24 and 25.

Figure 6. Aspen Plus model of selective non-catalytic reduction (SNCR).

isothermal assumption allows the process to be set at 1150 K (1610°F), which makes the SNCR process conditions uniform in terms of temperature between different systems being evaluated. If the incoming flue gas is not exactly at 1150 K (1610°F) the excess heat bypasses the SNCR reaction via the heat streams. In this way a space is created in the boiler where the conditions are right for SNCR simulating the way in which ammonia would be injected into selected areas of an actual boiler.

The amount of ammonia supplied to the process is controlled to avoid ammonia slip (un-reacted ammonia exiting the combustion unit). The reactions between ammonia, oxygen, and NO_x happen quickly according to the reaction mechanism presented in table 10.

Reactions 32 and 33 along with the kinetic parameters presented in table 11 come from the study Duo et al. (1992) where the reactions between NO and NH_3 in an atmosphere of excess O_2 are explored. This mechanism is suggested for use in modeling SNCR systems by Annamalai and Puri (2007).

Sulfur and Chlorine Emissions

The sulfur and chlorine found in the biomass fuels being evaluated have the potential to produce harmful air emissions of SO_x and HCl if not managed correctly. Fluidized bed combustors and gasifiers allow for the use of limestone as a bed material which helps to reduce SO_x and HCl emissions. Flue gas semi-dry scrubbers were also included to further reduce SO_x and HCl emissions.

Table 10. SNCR mechanism.[a]

No.	Reaction
32	$NH_3 + NO + \frac{1}{4}O_2 \rightarrow N_2 + \frac{3}{2}H_2O$
33	$NH_3 + \frac{5}{4}O_2 \rightarrow NO + \frac{3}{2}H_2O$

[a] Duo et al. (1992).

Table 11. SNCR mechanism kinetic parameters.[a]

No.	Rate Expression	Parameter (k)
32	$k[NH_3][NO]$	$2.45 \times 10^{14} \exp(-29400/T)$
33	$k[NH_3]$	$2.21 \times 10^{14} \exp(-38160/T)$

[a] All parameters are in SI units. Concentrations have units of [mol/ m³].
Duo et al. (1992).

The addition of limestone (calcium carbonate, $CaCO_3$) to a fluidized bed combustion process is a common method of reducing SO_x and HCl emissions (Desroches-Ducarne et al., 1998). In a combustion process most of the $CaCO_3$ bed material will be calcined to quicklime (CaO). The CaO will then be available to react with SO_2 to form solid $CaSO_4$ which can be removed with the ash. The CaO will also react with HCl to form solid $CaCl_2$ to be removed with the ash (Coda et al., 2001). This process occurs according to reactions 9, 10, and 11 as presented earlier in table 4.

Limestone can also be used in a fluidized bed gasifier to help capture sulfur and chlorine from the fuel (Yrjas et al., 1996). The interactions during gasification are somewhat similar to sorbent reactions during combustion. Some of the limestone added during gasification will form CaO, but this reaction will be limited by equilibrium conditions involving temperature and the concentration of CO_2 (Yrjas et al., 1996). The process considered for sulfur and chlorine capture is shown in reactions 21, 22, and 23 as presented earlier in table 7. Most fuel sulfur will form H_2S during gasification. CaO reacting with H_2S will form a solid CaS which is removed with the ash (Yrjas et al., 1996). HCl reacts with CaO to form solid $CaCl_2$ just as in the combustion cases (Weinell et al., 1992).

An additional method used to reduce emissions involving sulfur and chlorine is post combustion flue gas treatment. There are many options for flue gas treatment processes to capture sulfur and chlorine emissions after combustion. The method used in this research is a lime spray drying scrubber (or semi-dry lime scrubber).

In this process dry CaO is hydrated to form $Ca(OH)_2$ (hydrated lime) in a slaking process according to reaction 34 shown in table 12 (Black and Veatch, 1996). The hydrated lime is then mixed with more water to form slurry. The slurry is atomized into a spray dryer vessel where it reacts with the flue gas. The acid gases (SO_2 and HCl) are absorbed into the droplets and react to form salts. At the same time the moisture in the droplets is being evaporated to result in a dry by-product (Stein et al., 2002). The SO_2 in the flue gas reacts with the hydrated lime to form mainly calcium sulfite according to reaction 35 (Black and Veatch, 1996). HCl reacts with hydrated lime to form calcium chloride ($CaCl_2$) via reaction 36 (Stein et al., 2002).

Lime spray dryers are operated on an approach to adiabatic saturation temperature of the flue gas exiting the scrubber. Having the exit gas closer to the saturation

Table 12. Lime spray drying reactions.

No.[a]	Reaction
34	$CaO + H_2O \Leftrightarrow Ca(OH)_2$
35	$SO_2 + Ca(OH)_2 \Leftrightarrow CaSO_3 \cdot \frac{1}{2}H_2O + \frac{1}{2}H_2O$
36	$2HCl + Ca(OH)_2 \Leftrightarrow CaCl_2 \cdot 2H_2O$

[a] 34, 35: Black and Veatch (1996).
    36:    Stein et al. (2002).

temperature will result in higher reduction efficiencies because the process depends upon liquid phase reactions (Black and Veatch, 1996). However, the calcium chloride product becomes sticky if the process is too close to the saturation temperature (Black and Veatch, 1996). Systems ideally operate near an 11°C (20°F) temperature approach to saturation with a reagent ratio of 1.3 and obtain removal efficiencies of 90% for SO_x and higher removal efficiencies of HCl (Schnelle and Brown, 2002). For systems with significant amounts of HCl, this temperature approach is increased to 28°C or 56°C (50°F or 100°F) above saturation to avoid agglomeration of the solids (Schnelle and Brown, 2002). This increase in saturation temperature approach will decrease the reduction efficiency, but the presence of HCl in the system also works to increase the efficiency of SO_x reduction (Liu and Gibbs, 2002).

The lime spray dryer process is modeled in Aspen Plus by a series of RSTOICH reactors followed by an SSPLIT block which acts as a baghouse filter as shown in figure 7.

The model follows the reactions presented in table 12. Quicklime is reacted with excess water in the first step to form hydrated lime slurry. The slurry reacts with the flue gas in the next stage to remove acid gas components. The process is operated at a 42°C (75°F) temperature approach to saturation with a set 70% reduction of SO_x emissions and 85% reduction of HCl emissions based on the pollutant concentration entering the scrubber. A pressure drop of 1.1 kPa is assumed across the scrubber unit (Black and Veatch, 1996).
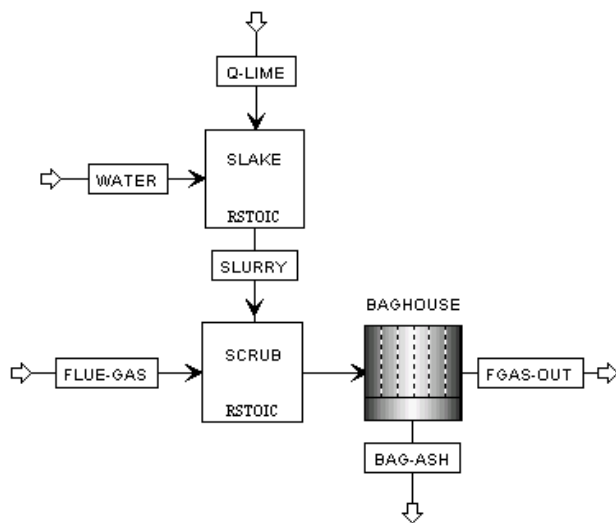
Figure 7. Aspen Plus model of lime spray drying scrubber.

Volatile Organic Compounds and Particulate Matter

In the coproduct drying process a small amount of VOCs are produced (Brady and Pratt, 2007). These compounds are regulated air pollutants and the dryer exhaust stream must be treated. All the models use steam tube dryers with the dryer exhaust being routed to the combustion unit where thermal oxidation occurs. The assumption made for modeling purposes is that the combustion reactor average temperature must be greater than 816°C (1500°F) to accomplish thermal oxidation of the VOCs (Lewandowski, 2000).

Emissions of particulate matter are not simulated in the analysis although the necessary particulate removal equipment is specified in each case. The particulate removal equipment (cyclones, baghouse, etc.) is specified using estimates from similar processes.

STEAM CYCLE AND ELECTRICITY PRODUCTION

Several variations of steam turbine power cycles were used to generate electricity in this analysis. Each fuel combination and technology scenario was analyzed on three levels of electricity production.

At the first level, the system simply provides the process heat needed to produce ethanol and dry the coproduct. No electricity is generated. Steam is generated at 1136 kPa (150 psig) for the coproduct dryer and ethanol process. However, the ethanol process uses steam at 446 kPa (50 psig), so a pressure-reducing valve is used to expand the steam before use. This is not the most thermodynamically efficient setup, but it is common in many ethanol plants because the industrial scale boilers are typically rated at pressures of 1136 kPa (150 psig) or above. This also makes ethanol plants good candidates for electricity production.

The second level system generates superheated steam at 482°C (900°F) and 6,300 kPa (900 psig) and uses a backpressure turbine to produce electricity. The limiting factor for electricity production in this case is that all the outlet steam from the turbine needs to be used for ethanol production and coproduct drying. Steam from the turbine outlet is used in the ethanol process and coproduct dryer at 446 kPa (50 psig). Under these constraints the actual amount of electricity produced always exceeds the ethanol plant requirements so some electricity is available to sell to the grid. The second level of electricity production is referred to as CHP (Combined Heat and Power).

At the third level a surplus of steam is generated at 482°C (900°F) and 6,300 kPa (900 psig) and is used to drive extraction type turbines. The steam necessary for ethanol production and coproduct drying is extracted at 446 kPa (50 psig) after the high pressure turbine stage and the excess steam is sent through the low pressure turbine stage then condensed. The amount of fuel used in this third level is limited to the amount of energy available if all the ethanol coproducts at the plant are used as fuel. At this level a portion of the electricity generated is used to meet the plant needs, and a significant amount of electricity is also sold to the grid.

RESULTS

Three combinations of fuel and thermal conversion technology are analyzed, each at the three different levels of electricity generation. For each case system performance results are presented.
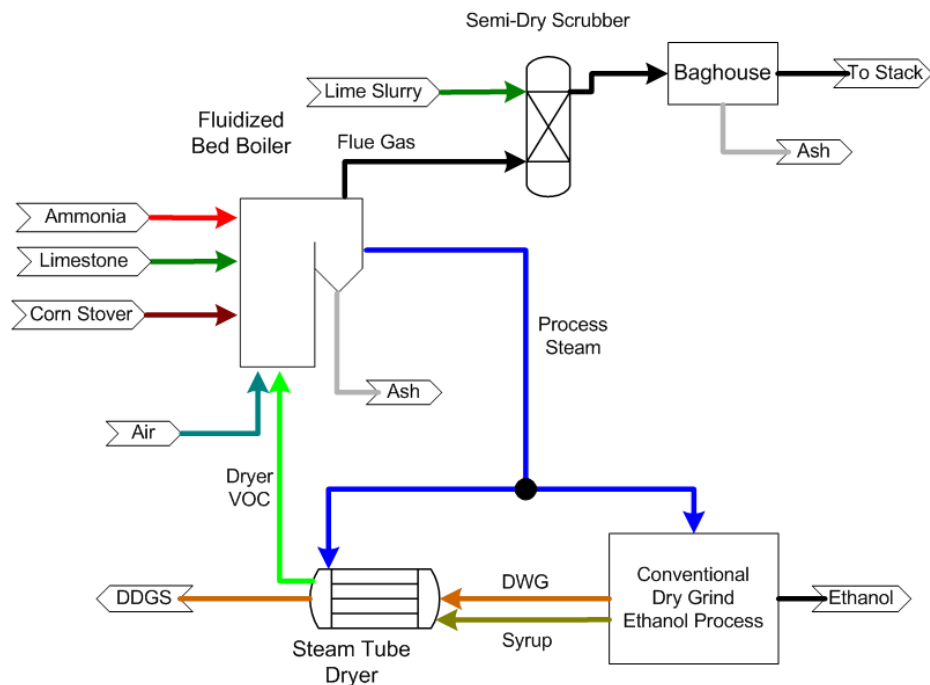
Figure 8. Corn stover combustion, level 1: Process heat only.

CORN STOVER COMBUSTION

The first option analyzed is the direct combustion of corn stover in a fluidized bed. The corn stover is assumed to be densified at an off-site facility. Figure 8 shows a simplified process flow diagram of this case. At the heart of the process is the bubbling fluidized bed boiler. The dryer exhaust stream is routed through the combustor to accomplish thermal oxidation of the volatile organic compounds it contains. Oxides of nitrogen are controlled using SNCR at the boiler. Limestone is added in the fluidized bed and the flue gas passes through a semi-dry scrubber to control SO_x and HCl. Particulate matter is removed from the flue gas by cyclones and a baghouse.

At the first level no electricity is generated. Saturated steam is produced in the boiler at 1136 kPa (150 psig) and then reduced to 446 kPa (50 psig) for use in ethanol processing and coproduct drying (see fig. 8).

At the second level electricity is generated using a backpressure turbine. Steam is produced at 6300 kPa (900 psig) and 482°C (900°F), then expanded through a backpressure turbine to 446 kPa (50 psig) (see fig. 9). Some de-superheating is then necessary to provide saturated steam to the ethanol process and the coproduct dryer.

The third level of electricity production uses an extraction turbine. A surplus of steam is generated in the boiler at 6300 kPa (900 psig) and 482°C (900°F). Process steam is extracted from the turbine at 446 kPa (50 psig) (see fig. 10). The remaining steam continues into the condensing stage where it expands to a final pressure of 10 kPa (13.2 psi lower than atmospheric pressure).

SYRUP AND CORN STOVER COMBUSTION

The next option analyzed is combustion of the syrup coproduct supplemented with corn stover. The process flow diagram for this system (shown in fig. 11) is essentially the same as the corn stover combustion case except that the syrup coproduct is not dried, but rather combusted in the fluidized

bed boiler along with corn stover. The drying operation in this case is much smaller because only the DWG coproduct must be dried. The process steam load is 12.8 MW$_{th}$ for drying only the DWG to produce DDG compared to 22.8 MW$_{th}$ for drying the DWG and syrup together to produce DDGS for a 190 million-L (50 million-gal) per year capacity plant. The amount of DDG produced is 59% of the amount of DDGS that would be produced if all of syrup were included in the dried coproduct.

The three levels of electricity production for this fuel combination follow the same iterations as the corn stover combustion cases discussed previously. Figure 11 shows a process flow diagram for the second level of electricity production. For all three levels all of the syrup produced at the plant is used as fuel. Figure 12 shows fuel energy input from syrup and corn stover for each level at 190 million-L (50 million-gal) per year capacity. The amount of fuel used is shown in figure 13. The average moisture contents of the fuel mixtures for the process heat, CHP, and CHP + grid scenarios are 55%, 52%, and 44%, respectively.

DDGS GASIFICATION

The last option analyzed is the gasification of DDGS (fig. 14). The system chosen uses an air-blown fluidized bed gasifier to convert the DDGS into synthesis gas. Particulates are removed from the gas stream in high-temperature cyclones. The synthesis gas is not allowed to cool significantly in order to avoid condensation of tars. A staged combustion reactor is used to combust the synthesis gas. Ambient air and exhaust from the DDGS dryer are added at separate stages. This combustion reactor acts as a thermal oxidizer for the dryer exhaust stream and eliminates that capital expense. Immediately following the combustor is a heat recovery steam generator (HRSG) where steam is produced for the ethanol process, coproduct drying, and electricity production depending on the specific case. SNCR is used to reduce NO$_x$ emissions. Limestone is added in the
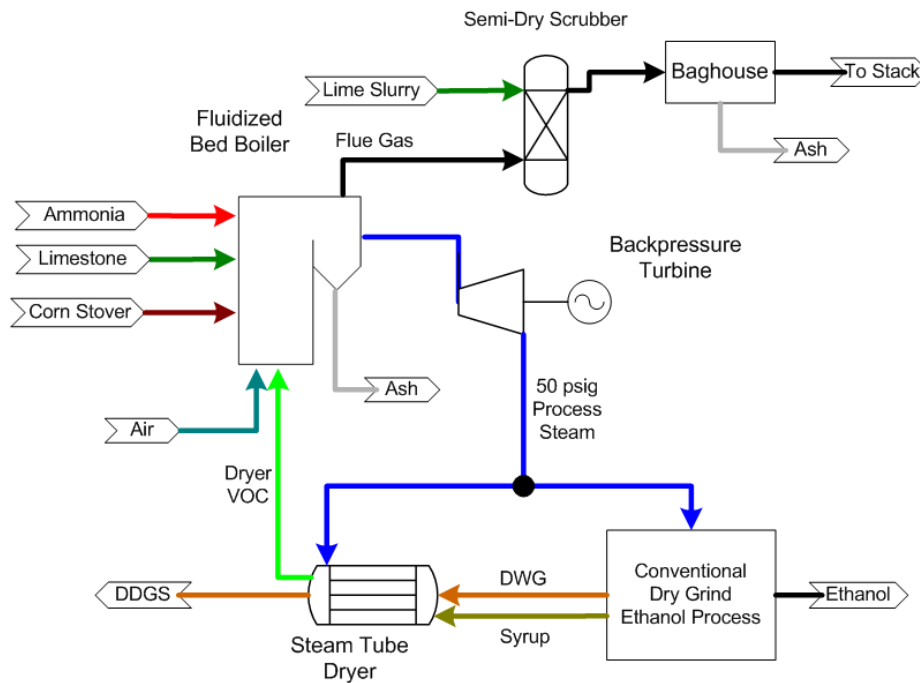
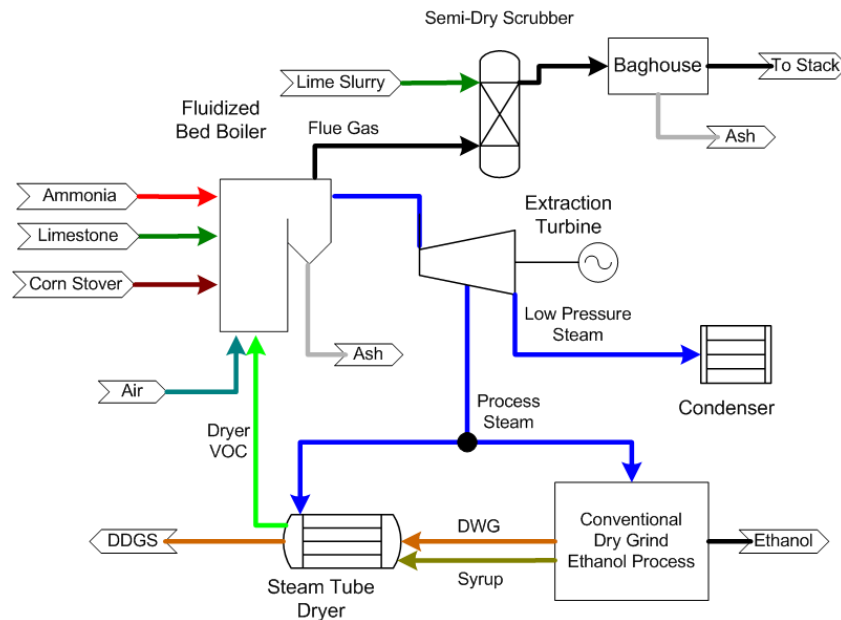**Figure 9. Corn stover combustion, level 2: CHP.**

Figure 10. Corn stover combustion, level 3: CHP and electricity to the grid.

fluidized bed gasifier and the flue gas passes through a semi-dry scrubber to control SO_x and HCl.

The second level of electricity production for the DDGS gasification option is shown in figure 14. The other levels of electricity production have system changes similar to the previously mentioned cases of corn stover combustion.

Gasification of DDGS is an attractive option because of relatively low temperature ash fusion characteristics of DDGS. The gasification reaction occurs at lower temperatures than combustion and much of the ash is removed before the gas is combusted. This decreases the chance of fouling the boiler tubes with alkali deposits.

SYSTEM PERFORMANCE COMPARISONS

Table 13 presents some of the performance data of interest from each case. The maximum fuel energy input rate (level three - CHP + Grid) is set at the total amount of energy available in the ethanol coproducts. So, in the case of DDGS gasification all of the DDGS is used as fuel and the ethanol plant produces no other coproduct for sale. The other two fuel scenarios (corn stover, and syrup and corn stover) are set at the same maximum thermal fuel input rate to facilitate comparisons.

The use and generation of electricity varies significantly between the systems. For process heat only, the power is negative since electricity is purchased from the local utility.
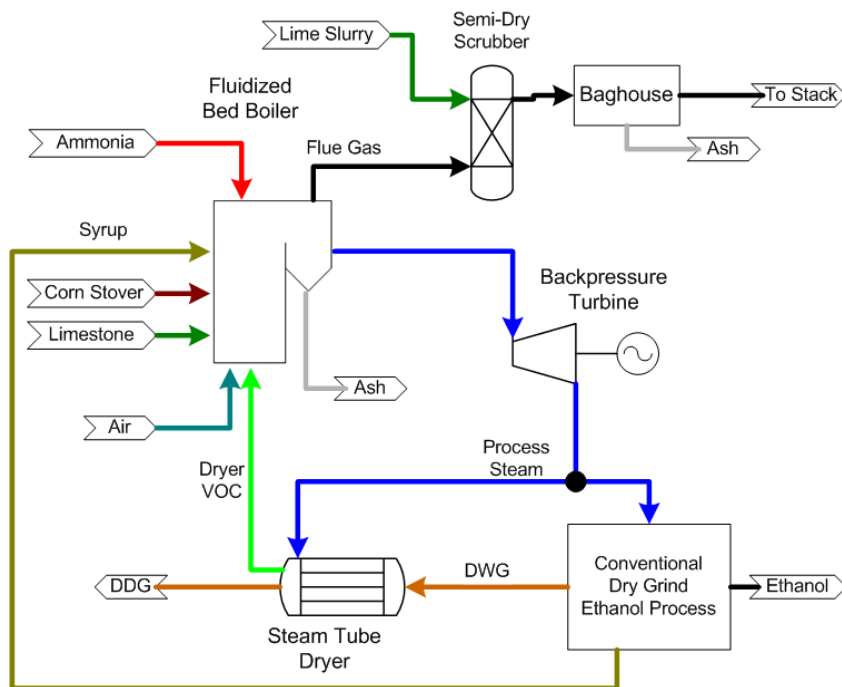
Figure 11. Syrup and corn stover combustion, level 2: CHP.

Power above zero is generated at the ethanol plant (CHP and CHP + Grid), some of which is used with the surplus being sent to the power grid. At level 2 (CHP), corn stover combustion and DDGS gasification generate approximately the same amount of power (10.9 MW$_e$), because they are both dry fuels and the ethanol plant process load and the DDGS dryer load are the same for both cases. For the syrup and corn stover CHP case, less process steam is required for drying the coproduct since only DWG is being dried. This limits the amount of steam flowing through the backpressure turbine and, therefore power produced, since all of the output steam must be used to meet process needs. Syrup moisture is vaporized in the combustor where it decreases the boiler efficiency rather than being evaporated in the dryer via process steam where it could provide additional load for the back pressure turbine. Power produced at level three (CHP + Grid) increases compared to level two (CHP) because excess steam is run through a condensing turbine. Corn stover combustion produces the largest amount of power, followed by syrup and corn stover combustion, and then DDGS gasification. Although both fuels are dry, DDGS gasification produces less power than corn stover combustion because of

internal losses such as unreacted carbon and heat loss from the producer gas before it is combusted.

There is a moderate increase in power generation efficiency between the level two (CHP) and level three (CHP + grid) cases (table 13). The difference between levels two and three is an improvement in the Rankine power cycle. The excess steam being condensed at low pressure effectively increases the difference in high and low temperatures of the system, making higher generation efficiencies possible.

The system thermal efficiency is a measure of how effectively the fuel energy supplied to produce heat and power is used. The process heat and CHP systems have similar thermal efficiencies (table 13). In the CHP + grid cases, excess steam is produced and a significant amount of heat is lost to the atmosphere in the condenser resulting in lower system thermal efficiencies. In general, the combustion of corn stover makes the most efficient use of the fuel energy input due to its simplicity and relatively low fuel moisture content. The gasification cases are lower than the corn stover combustion cases because of internal losses as described above. Syrup and corn stover combustion cases
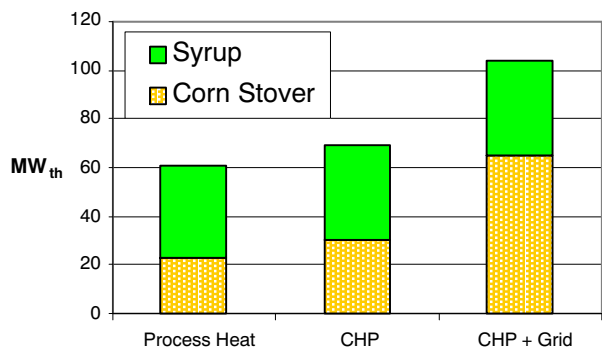

Figure 12. Syrup and corn stover combustion: fuel energy input rate contribution (HHV).
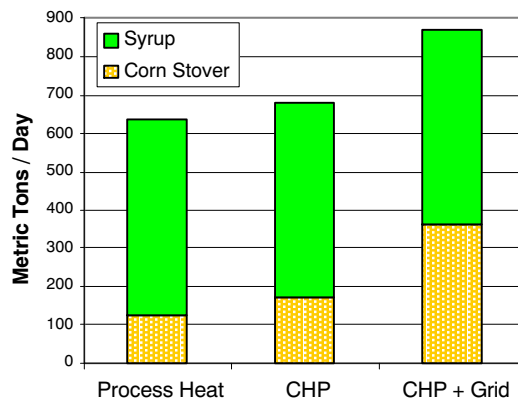

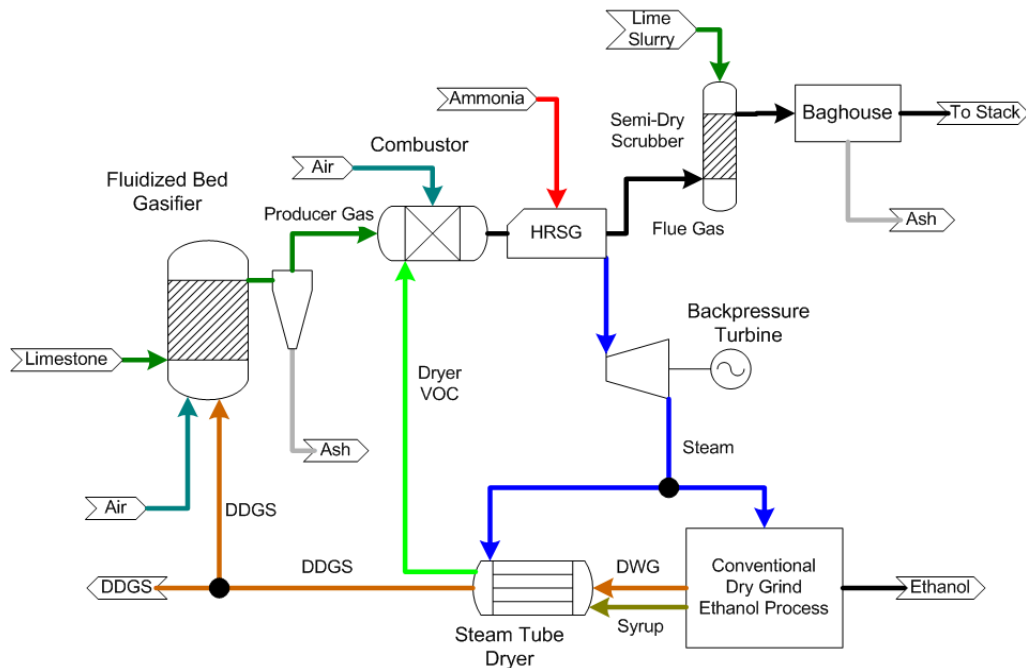**Figure 13. Syrup and corn stover combustion: fuel use.**

Figure 14. DDGS gasification, level 2: CHP.

have the lowest system thermal efficiencies, because as described above the syrup moisture is vaporized in the combustor rather than in the dryer via process steam where the energy would be counted as a useful output of the system.

Ethanol coproducts have advantages as fuels because they are available at the plant. However, if they are used for fuel less is available to sell as livestock feed. Corn stover does not compete with the livestock feed use, but it is not available at the plant so extra costs are incurred in procuring it as a fuel. The syrup and corn stover option preserves the higher protein portion (dried DWG or DDG) for sale, while using the lower feed value syrup as fuel. This reduces the amount of corn stover required by 40% to 65% depending on the level of electricity generation. The choice of fuel will depend on an economic analysis, which is underway.

Control of NO_x, SO_x, and HCl emissions are essential for successful implementation of biomass-fueled ethanol plants. Stack emissions results with control technologies in place for NO_x are presented in table 14. The biomass fuels contain significant amounts of nitrogen. This fuel nitrogen has the potential to result in NO_x during the thermo-chemical conversion process. The amount of fuel nitrogen that is converted to NO_x depends on the conditions present in the gasification and combustion steps such as the reaction temperature and the amount of oxygen present. The corn stover combustion cases have the highest percentage of fuel nitrogen converted to NO_x. This is due in part to the higher reaction temperatures of these cases (927°C for corn stover combustion compared to 900°C in the other combustion cases). The high conversion of fuel nitrogen to NO_x can also

Table 13. System performance results for a 190 million-L (50 million-gal) per year dry-grind ethanol plant[a].

	Biomass Fuel Use[b] (Wet Basis) (t/day)	Fuel Energy Input Rate (MW$_{th}$)	Power Generated (Gross) (MW$_e$)	Power To Grid (Net)[c] (MW$_e$)	Power Generation Efficiency (%)	System Thermal Efficiency[d] (%)
Corn stover combustion						
Level 1: Process heat only	355	64.1	0	-6.0	–	77.1
Level 2: CHP	431	77.9	10.9	4.6	14.0	77.0
Level 3: CHP & elec. to grid	575	103.9	17.4	10.7	16.7	63.6
Syrup & corn stover combustion						
Level 1: Process heat only	647	63.6	0	-5.7	–	62.4
Level 2: CHP	709	74.8	8.8	2.8	11.8	64.5
Level 3: CHP & elec. to grid	870	103.9	16.0	9.6	15.4	53.0
DDGS gasification						
Level 1: Process heat only	307	69.6	0	-5.4	–	71.9
Level 2: CHP	374	84.5	10.9	5.2	12.9	71.7
Level 3: CHP & elec. to grid	459	103.9	15.4	9.6	14.8	62.5

[a] All energy and power values in this table are based on the fuel Higher Heating Value (HHV).
[b] Moisture contents: Corn stover - 13%; Syrup & corn stover - 55%, 52%, 44% for levels 1, 2, 3, respectively; DDGS - 10%.
[c] Negative values refer to power purchased from the grid by the ethanol facility.
[d] Efficiency of converting fuel energy into other useful forms of energy (process heat and electricity).

be explained by the relatively small amount of nitrogen present in corn stover. Annamalai and Puri (2007) present data from Pohl and Sarofim (1976) which shows that the percent conversion of fuel nitrogen to NO_x decreases as the weight percent of nitrogen in the fuel increases for a variety of coal and oil fuels. Corn stover has about one seventh of the nitrogen of DDGS and about one quarter of the nitrogen found in syrup (table 3). It is reasonable then, that corn stover with its low nitrogen content would convert a larger fraction of this nitrogen to NO_x during combustion compared to the other fuel combinations.

In the cases where syrup is combusted a lower amount of fuel nitrogen ends up as NO_x. This is partially because the reaction temperature is lower than that of corn stover combustion and the evaporation of the moisture in the syrup absorbs heat. It is also due to the fact that syrup contains much more fuel nitrogen than corn stover, so a smaller fraction of nitrogen ends up as NO_x following the trend mentioned above.

The fuel nitrogen interactions in the DDGS gasification cases are different because the synthesis gas combustion is modeled in a staged configuration. During gasification fuel nitrogen is assumed to devolatilize as NH_3 and HCN forming part of the synthesis gas. In the first stage of synthesis gas combustion the dryer exhaust stream serves as the source of oxidizer. In the second stage of synthesis gas combustion additional combustion air is added to the partially combusted synthesis gas. More details of this process are presented in De Kam (2008).

All cases use SNCR ammonia injection to reduce NO_x emissions. NH_3 is injected into the flue gas at a point in the boiler after the combustion reaction where the temperature has dropped to 877°C. NO_x emissions are reduced by 40% to 70% depending on the specific case as shown in table 14.

The final emissions of NO_x are highest in the DDGS gasification cases despite the fact that this system is the most effective at mitigating the conversion of fuel nitrogen into NO_x. These higher emissions are due to the very high nitrogen content of the DDGS fuel. This same gasification system using corn stover as a fuel would almost certainly have lower NO_x emissions than the corn stover combustion systems. NO_x emissions from the syrup combustion cases generally decrease as the size of the system gets larger because syrup is the main source of nitrogen and the supplementary fuels provide more energy without the added fuel nitrogen.

None of the NO_x annual emissions rates are above the current regulatory threshold of 227 metric tons (250 tons) per year which would put them in the major source category (EPA, 2006). If plant capacities were expanded to 380 million L (100 million gal) per year, many of the cases would exceed the major source regulatory threshold for NO_x. This threshold is not a limit, but a plant that is over this amount will have to comply with a more rigorous permitting process.

Some of the biomass fuels considered in this study contain significant amounts of sulfur, especially the ethanol coproducts. This high sulfur content creates potential for SO_x emissions. Two technologies for sulfur capture are used in each system. The sulfur capture rates and SO_x emissions results are shown in table 15.

The first method of capturing sulfur is to add limestone sorbent material in the fluidized bed reactors. The amount of sulfur captured by limestone in the fluidized bed depends on the reaction temperature and the calcium to sulfur ratio. Since this Ca/S ratio is fixed at 3 for all cases the differences in capture are due mostly to temperature. Black and Veatch (1996) show that the best temperature for sulfur capture in fluidized bed combustors is near 840°C. The cases that combust syrup operate closer to this temperature and therefore have better capture rates than the corn stover combustion cases. The ability of limestone to absorb sulfur is diminished in a gasification atmosphere, so it follows that the DDGS gasification cases capture less sulfur in the fluidized bed sorbent.

The second emissions control technology used to capture sulfur is lime spray drying semi-dry scrubbers. The scrubbers are modeled under the same operating conditions for all cases, so the main determining factor for sulfur capture is the concentration of SO_2 entering the scrubber. The combination of these two sulfur capture technologies results in a high rate of sulfur capture in all of the cases. The final emission rates of sulfur reflect these reduction rates and also the relative amount of sulfur in the fuel being used.

Table 14. Emissions of NOx after control technology for a 190 million-L (50 million-gal) per year dry-grind ethanol plant[a].

	Fuel N Converted to NO_x, %	SNCR NO_x Reduction Efficiency[b], %	NO_x Emissions Rate[c]		NO_x Annual Emissions	
			g/MJ	(lb/MMBtu)	t/yr	(tn/yr)
Corn stover combustion						
Level 1: Process heat only	6.3	40	0.05	(0.11)	96	(106)
Level 2: CHP	7.8	47	0.05	(0.12)	128	(142)
Level 3: CHP & elec. to grid	8.5	53	0.05	(0.12)	163	(179)
Syrup & corn stover combustion						
Level 1: Process heat only	4.5	60	0.06	(0.13)	113	(124)
Level 2: CHP	4.8	61	0.05	(0.13)	127	(140)
Level 3: CHP & elec. to grid	5.4	62	0.05	(0.12)	163	(179)
DDGS Gasification						
Level 1: Process heat only	1.6	48	0.06	(0.14)	131	(144)
Level 2: CHP	2.4	61	0.07	(0.16)	181	(199)
Level 3: CHP & elec. to grid	3.1	70	0.07	(0.15)	214	(236)

[a] All NO_x emissions are calculated as NO_2.
[b] Emissions controls include selective non-catalytic reduction (SNCR) in all cases plus staged combustion for DDGS gasification.
[c] Values are based on the fuel Higher Heating Value (HHV).

Table 15. Emissions of SOx after control technology for a 190 million-L (50 million-gal) per year dry-grind ethanol plant[a].

	SO_x Emissions Capture Efficiency[b] (%)	SO_x Emissions Rate[c]		SO_x Annual Emissions	
		g/MJ	(lb/MMBtu)	t/yr	(tn/yr)
Corn stover combustion					
Level 1: Process heat only	86	0.006	(0.015)	13	(14)
Level 2: CHP	87	0.006	(0.014)	14	(16)
Level 3: CHP & elec. to grid	88	0.005	(0.012)	17	(19)
Syrup & corn stover combustion					
Level 1: Process heat only	90	0.059	(0.14)	119	(131)
Level 2: CHP	89	0.056	(0.13)	131	(144)
Level 3: CHP & elec. to grid	87	0.050	(0.12)	163	(179)
DDGS Gasification					
Level 1: Process heat only	91	0.065	(0.15)	144	(159)
Level 2: CHP	91	0.065	(0.15)	173	(191)
Level 3: CHP & elec. to grid	91	0.065	(0.15)	213	(235)

[a] All SO_x emissions are calculated as SO_2.
[b] Emission controls include limestone sorbent in the fluidized bed (combustion and gasification) plus flue-gas semi-dry scrubbers in all cases.
[c] Values are based on the fuel Higher Heating Value (HHV).

The annual emission rates for SO_x are below the EPA major source threshold for criteria pollutants of 227 tonnes (250 tons) per year for all cases for this size plant, which means they may qualify for a simpler air emissions permitting process. The emission rates for SO_x in the corn stover combustion cases are small because corn stover contains very little sulfur.

Chlorine emissions in the form of HCl are a problem associated with many biomass fuels including those being evaluated in this study. The same control technologies used to capture sulfur are used for chlorine capture in these systems. A summary of chlorine capture and emissions results is shown in table 16. For the combustion cases the majority of chlorine is captured in the fluidized bed sorbent. The limestone sorbent is less effective in a gasification atmosphere resulting in less sorbent capture for the DDGS gasification cases. The ability of the lime spray drying scrubber to capture HCl is very good in general and depends on the incoming concentration of HCl. The combined chlorine capture rates are quite high using these two control technologies. The EPA major source threshold for annual emissions of HCl, which is hazardous air pollutants, is 9 tonnes (10 tons) per year. The DDGS gasification cases are well above this level due to the low amount of chlorine capture happening in the gasifier bed sorbent. Even with the higher capture rates for chlorine, the cases involving combustion of syrup are near or above the major source threshold. The emission rates for HCl in the corn stover combustion cases are well below the major source threshold because corn stover contains less chlorine than the ethanol coproducts.

We used our models to estimate electricity generation, use, and amount to the grid for biomass plants (table 17). The amount of electricity needed in biomass-powered plants increases as a result of the additional equipment, such as fluidized beds and semi-dry scrubbers, required to successfully use these fuels. However, up to 0.73 kWh/L (2.75 kWh/gal) of renewable electricity can be generated with up to 0.45 kWh/L (1.69 kWh/gal) sent to the grid.

Table 16. Emissions of chlorine after control technology for a 190 million-L (50 million-gal) per year dry-grind ethanol plant[a].

	HCl Emissions Capture Efficiency[b] (%)	HCl Emissions Rate[c]		HCl Annual Emissions	
		g/MJ	(lb/MMBtu)	t/yr	(tn/yr)
Corn stover combustion					
Level 1: Process heat only	97	0.002	(0.005)	4.0	(4.4)
Level 2: CHP	97	0.002	(0.004)	4.3	(4.8)
Level 3: CHP & elec. to grid	97	0.002	(0.004)	5.0	(5.6)
Syrup & corn stover combustion					
Level 1: Process heat only	97	0.004	(0.010)	8.3	(9.2)
Level 2: CHP	97	0.004	(0.009)	9.0	(9.9)
Level 3: CHP & elec. to grid	97	0.003	(0.008)	10.7	(11.8)
DDGS gasification					
Level 1: Process heat only	89	0.009	(0.21)	20.5	(22.5)
Level 2: CHP	89	0.009	(0.21)	24.6	(27.1)
Level 3: CHP & elec. to grid	89	0.009	(0.21)	30.2	(33.3)

[a] All chlorine emissions are calculated as HCl.
[b] Emission controls include limestone sorbent in the fluidized bed (combustion and gasification) plus flue-gas semi-dry scrubbers in all cases.
[c] Values are based on the fuel Higher Heating Value (HHV).

Table 17. Electricity generation, use, and amount to the grid for conventional and biomass fueled plants [kWh/L (kWh/gal)].

	Electricity Generated, kWh/L (kWh/gal)	Electricity Used, kWh/L (kWh/gal)	Electricity to Grid, kWh/L (kWh/gal)
Conventional natural gas			
Level 1: Process heat only	0	0.20 (0.75)	0
Corn stover combustion			
Level 1: Process heat only	0	0.25 (0.94)	0
Level 2: CHP	0.45 (1.72)	0.26 (1.00)	0.19 (0.72)
Level 3: CHP & elec. to grid	0.73 (2.75)	0.28 (1.06)	0.45 (1.69)
Syrup & corn stover combustion			
Level 1: Process heat only	0	0.24 (0.91)	0
Level 2: CHP	0.37 (1.39)	0.25 (0.96)	0.12 (0.44)
Level 3: CHP & elec. to grid	0.67 (2.54)	0.27 (1.02)	0.40 (1.52)
DDGS Gasification			
Level 1: Process heat only	0	0.22 (0.85)	0
Level 2: CHP	0.46 (1.73)	0.24 (0.90)	0.22 (0.83)
Level 3: CHP & elec. to grid	0.64 (2.44)	0.25 (0.93)	0.40 (1.51)

Figure 15 shows the comparison of renewable energy ratio between the modeled cases and a conventional dry-grind corn ethanol plant. The calculations are based on equation 1, appropriate estimates from table 2, and fossil energy reductions for process heat and/or fossil electrical energy replaced or renewable electrical energy generated for the various biomass cases. It can be seen that using biomass as a fuel can greatly increase the renewable energy balance of ethanol production. Electricity generation further increases the renewable energy balance. A complete life-cycle analysis of the impact on greenhouse gas (GHG) emissions of substituting biomass fuels for fossil energy use at the plant is underway. However, the significant increases in renewable energy ratio provide a good indication of the potential reductions in life-cycle GHG emissions possible for the various biomass cases.

CONCLUSIONS

The results show that ethanol plants are a prime candidate for biomass combined heat and power systems. The CHP systems which produce only the amount of steam necessary to meet process needs are the best option for implementation at ethanol plants. These systems have the highest thermal efficiencies of all the cases evaluated and provide substantial improvements in the renewable energy balance of ethanol production with moderate added complexity.

The emissions estimates demonstrate that these biomass materials, particularly the ethanol coproducts, present challenges when used as fuel, but these challenges can be met using proper emissions control equipment. Fluidized bed combustors and gasifiers are important for use with these biomass fuels because of the sulfur and chlorine capture possible by adding limestone to the bed material. Staged synthesis gas combustion helps reduce NO_x emissions, particularly for DDGS, which has high nitrogen levels. Utilizing DDGS as a fuel is particularly challenging due to the high nitrogen, chlorine, and sulfur content as well as the low ash fusion temperatures. Systems using the syrup coproduct as a fuel have less potential for emissions problems than the DDGS coproduct, but sulfur and chlorine are still a concern. Corn stover used alone as a fuel presents fewer potential emissions issues than either of the ethanol coproducts.

Using biomass to provide heat and power at ethanol plants can improve the renewable energy ratio of ethanol production significantly. While a well-designed conventional natural gas fired ethanol facility may have a renewable energy ratio of 1.7, using biomass to provide process heat or process heat and electricity could improve this ratio to between 2.7 and 4.7.
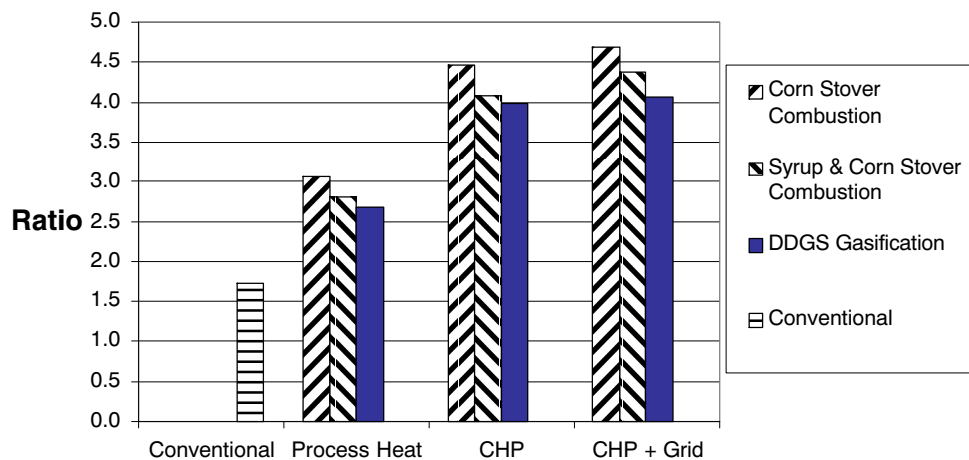
Figure 15. Renewable energy ratio (LHV).

REFERENCES

Annamalai, K., and I. K. Puri. 2007. *Combustion Science and Engineering.* Boca Raton, Fla.: CRC Press.

Anon. 2008. Steam tube dryers. Davenport Dryer Company. Available at: www.davenportdryer.com.

Babcock & Wilcox Co. 1992. *Steam: Its Generation and Use.* 40th ed., eds. J. B. Kitto, and S. C. Stultz. Baberton, Ohio: Babcock & Wilcox.

Black & Veatch. 1996. *Power Plant Engineering,* eds. L. Drbal, K. Westra, and P. Boston. New York, N.Y.: Chapman & Hall.

Belyea, R. L., K. D. Rausch, and M. E. Tumbleson. 2004. Composition of corn and distillers dried grains with solubles from dry grind ethanol processing. *Bioresource Tech.* 94(3): 293-298.

Brady, D., and G. C. Pratt. 2007. Volatile organic compound emissions from dry mill ethanol production. *J. Air and Waste Mgmt. Assoc.* 57(9): 1091-1102.

Chejne, F., and J. P. Hernandez. 2002. Modeling and simulation of coal gasification process in fluidized bed. *Fuel* 81(13): 1687-1702.

Ciferno, J. P., and J. J. Marano. 2002. Benchmarking biomass gasification technologies for fuels, chemicals, and hydrogen production. Pittsburgh, Pa.: National Energy Technology Laboratory. United States Dept. of Energy. Available at: 204.154.137.14/technologies/coalpower/gasification/pubs/pdf/BMassGasFinal.pdf.

Coda, B., M. Aho, R. Berger, and K. R. G. Hein. 2001. Behavior of chlorine and enrichment of risky elements in bubbling fluidized bed combustion of biomass and waste assisted by additives. *Energy and Fuels* 15(3): 680-690.

De Kam, M. J. 2008. Biomass combined heat and power for the ethanol industry. Unpublished M.S. thesis. Minneapolis, Minn.: University of Minnesota Library.

Desroches-Durcarne, E., J. C. Dolignier, E. Marty, G. Martin, and L. Delfosse. 1998. Modelling of gaseous pollutants emissions in circulating fluidized bed combustion of municipal refuse. *Fuel* 77(13): 1399-1410.

de Souza-Santos, M. L. 2004. *Solid Fuels Combustion and Gasification.* Monticello, N.Y.: Marcel Dekker.

Duo, W., K. Dam-Johansen, and K. Ostergaard. 1992. Kinetics of the gas-phase reaction between nitric oxide ammonia and oxygen. *The Canadian J. Chem. Eng.* 70(Oct): 1014-1020.

Duo, W., N. F. Kirby, J. P. K. Seville, J. H. A. Kiel, A. Bos, and H. Den Uil. 1996. Kinetics of HCl reactions with calcium and sodium sorbents for IGCC fuel gas cleaning. *Chem. Eng. Sci.* 51(11): 2541-2546.

EPA. 2005. Integration of VOC Destruction and CHP in the Ethanol Industry. Washington D.C.: Environmental Protection Agency. Available at: www.epa.gov/chp/markets/ethanol.html. Accessed May 2008.

EPA. 2006. Prevention of Significant Deterioration, Nonattainment New Source Review, and Title V: Treatment of Certain Ethanol Production Facilities Under the "Major Emitting Facility" Definition. EPA Docket ID No. EPA-HQ-OAR-2006-0089. Washington D.C.: Environmental Protection Agency.

EPA. 2007. Impact of Combined Heat and Power on Energy Use and Carbon Emissions in the Dry Mill Ethanol Process. Washington D.C.: Environmental Protection Agency. Available at: www.epa.gov/chp/markets/ethanol.html.

Higman, C., and M. van der Burgt. 2003. *Gasification.* Burlington, Mass.: Elsevier Science.

Khan, A. A., W. De Jong, D. R. Gort, and H. Spliethoff. 2007. A fluidized bed biomass combustion model with discretized population balance: 1. Sensitivity analysis. *Energy and Fuels* 21(4): 2346-2356.

Klass, D. L. 1998. *Biomass for Renewable Energy, Fuels, and Chemicals.* San Diego, Calif.: Academic Press.

Kwiatkowski, J. R., A. J. McAloon, F. Taylor, and D. B. Johnston. 2006. Modeling the process and costs of fuel ethanol production by the corn dry-grind process. *Ind. Crops and Products* 23(3): 288-296.

Lewandowski, D. A. 2000. *Design of Thermal Oxidation Systems for Volatile Organic Compounds.* Boca Raton, Fla.: CRC Press.

Liu, H., and B. M. Gibbs. 2002. Modelling of NO and N_2O emissions from biomass-fired circulating fluidized bed combustors. *Fuel* 81(3): 271-280.

Liu, H., and B. M. Gibbs. 2003. Modelling of NH_3 and HCN emissions from biomass circulating fluidized bed gasifiers. *Fuel* 82(13): 1591-1604.

McAloon, A. J., F. Taylor, W. C. Yee, K. Ibsen, and R. Wooly. 2000. Determining the cost of producing ethanol from corn starch and lignocellulosic feedstocks. NREL/TP-580-28893. Golden, Colo.: National Renewable Energy Laboratory.

McAloon, A. J., F. Taylor, and W. C. Yee. 2004. A model of the production of ethanol by the dry grind process. In *Proc. of the Corn Utilization & Technology Conf.* Indianapolis, Ind.: National Corn Growers Association and Corn Refiners Association.

Melgar, A., J. F. Pérez, H. Laget, and A. Horillo. 2007. Thermochemical equilibrium modeling of a gasifying process. *Energy Conversion and Mgmt.* 48(1): 59-67.

Morey, R. V., D. G. Tiffany, and D. L. Hatfield. 2006. Biomass for electricity and process heat at ethanol plants. *Applied Eng. in Agric.* 22(5): 723-728.

Morey, R. V., D. L. Hatfield, R. Sears, D. Haak, D. G. Tiffany, and N. Kaliyan. 2009. Fuel properties of biomass feed streams at ethanol plants. *Applied Eng. in Agric.* 25(1): 57-64.

Ngampradit, N., P. Plumsomboon, and B. Sajjakulnukit. 2004. Simulation of a circulating fluidized bed combustor with shrinking core and emissions models. *ScienceAsia* 30(4): 365-374.

Nikoo, M. B., and N. Mahinpey. 2008. Simulation of biomass gasification in fluidized bed reactor using Aspen Plus. *Biomass and Bioenergy* 32(12): 1245-1254.

Perry, R. H., J. O. Maloney, and D. W. Green. 1997. *Perry's Chemical Engineer's Handbook,* 7th ed. New York, N.Y.: McGraw-Hill.

Pohl, J. H., and A. F. Sarofim. 1976. In *Proc. of the Stationary Source Combustion Symposium.* EPA report 600-12-76-15a. Paper #GT2003-38294. Washington, D.C.: EPA.

Radovanović, M. 1986. *Fluidized Bed Combustion.* New York, N.Y.: Hemisphere Publishing Corporation.

Rausch, K. D., and R. L. Belyea. 2006. The future of coproducts from corn processing. *Appl. Biochem. and Biotech.* 128: 47-86.

Rosentrater, K. A. 2006. Some physical properties of distillers dried grains with solubles (DDGS). *Applied Eng. in Agric.* 22(4): 589-595.

Ruggiero, M., and G. Manfrida. 1999. An equilibrium model for biomass gasification processes. *Renewable Energy* 16(1-4): 1106-1109.

Schnelle, K. B., and C. A. Brown. 2002. *Air Pollution Control Technology Handbook.* Boca Raton, Fla.: CRC Press.

Shapouri., H., J. A. Duffield, and M. Wang. 2002. The energy balance of corn ethanol: An update. Agricultural Economic Report No. 813. Washington, D.C.: USDA.

Shapouri, H., J. Duffield, A. McAloon, and M. Wang. 2004. The 2001 net energy balance of corn-ethanol (preliminary). Washington, D.C.: USDA, Office of the Chief Economist.

Soave, G. 1972. Equilibrium constants for modified Redlich-Kwong Equation-of-state. *Chem. Eng. Sci.* 27(6): 1197-1203.

Sokhansanj, S., and A. F. Turhollow. 2004. Biomass densification-cubing operations and costs for corn stover. *Applied Eng. in Agric.* 20(4): 495-499.

Stein, J., M. Kind, and E. Schlunder. 2002. The influence of HCl on SO$_2$ absorption in the spray dry scrubbing process. *Chem. Eng. J.* 86(1-2): 17-23.

Turns, S. R. 2000. *An Introduction to Combustion*. Boston, Mass.: McGraw-Hill.

Wang, M., M. Wu, and H. Huo. 2007. Life-cycle energy and greenhouse gas emission impacts of different corn ethanol plant types. *Environ. Res. Letters* 2(2): 024001.

Weinell, C. E., P. I. Jensen, K. Dam-Johansen, and H. Livbjerg. 1992. Hydrogen chloride reaction with lime and limestone: Kinetics and sorption capacity. *Ind. and Eng. Chem. Res.* 31(1): 164-171.

Wooley, R. J., and V. Putsche. 1996. Development of an ASPEN PLUS Physical Property Database for Biofuels Components. Golden, Colo.: National Renewable Energy Laboratory.

Yrjas, K. P., C. A. P. Zevenhoven, and M. M. Hupa. 1996. Hydrogen sulfide capture by limestone and dolomite at elevated pressure. *Ind. and Eng. Chem. Res.* 35(1): 176-183.